EUROPEAN ORGANIZATION FOR NUCLEAR RESEARCH
European Laboratory for Particle Physics

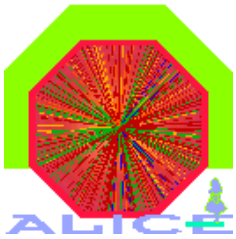

Internal Note/V0
ALICE reference number
ALICE-INT-2005-052 version 1.0
Institute reference number
[-]
Date of last change
November 11 2005

Radiation effects on V0 detector elements

Authors:

B. Cheynis, L. Ducroux, J.-Y. Grossiord, A. Guichard, P. Pillot,
B. Rapp, R. Tieulent, W. Tromeur, Y. Zoccarato
IPN-Lyon, IN2P3-CNRS et Université Claude Bernard, Lyon-I, France

Abstract:
The 60 MeV proton beam delivered by the RADEF facility of the University of Jyväskylä (Finland) was used to measure the radiation effects on a scintillator counter and on an electronics circuit prototype designed and built for the V0 detector of ALICE. The light yield and the time resolution given by a counter of the inner ring of the V0C array were measured as a function of the radiation dose up to about 300 krad. The number of Single Event Upsets (SEU) induced in a FPGA chip was determined as a function of the flux of particles expected during 10 years of ALICE running.

Contents

1 Introduction

The description of the V0 detector of ALICE can be found in the Technical Design Report [1]. It is a small-angle detector consisting of two arrays of 32 scintillator counters (named V0A and V0C) installed on both sides of the ALICE collision vertex. The counters cover the pseudo-rapidity ranges of $2.8 < \eta < 5.1$ (V0A) and $-3.7 < \eta < -1.7$ (V0C). The individual counter of the last array is made of two layers of 9 WLS fibres glued along the two radial edges of a scintillating piece and connected to two bundles of 9 optical fibres as shown in Fig. 1. The components used are a BC404 scintillator 2 cm thick, BCF9929A WLS fibres (double cladding) of 1 mm in diameter and BCF98 optical fibres (d.c.) of 1.1 mm in diameter.

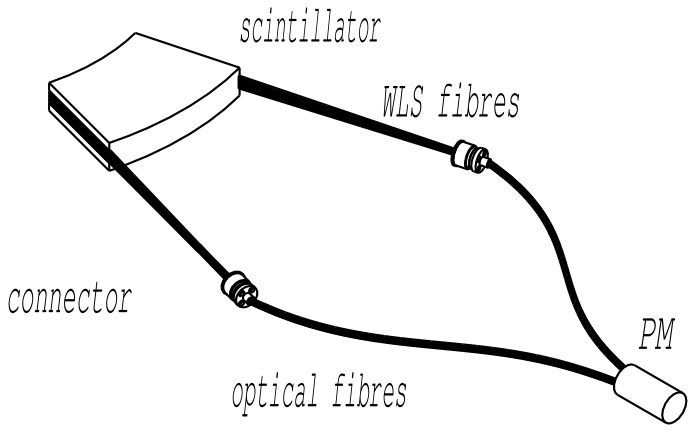

Figure 1: Elementary counter of the V0C array.

Amongst all the questions raised during the V0 development, there was the problem of radiations and their effects on the signal delivered by each channel of the detector on one hand, their effect on the electronics devices installed in the cavern close to the L3 magnet on the other hand. In order to get quantitative answers to these questions, we carried out several measurements with a 60 MeV proton beam delivered by the Jyväskylä RADEF facility. They included:

- radiation ageing effect on the elements constituting the individual counter of the V0C array (Section 2). Similar tests were carried out on the same scintillating elements in the frame of the design adopted for the V0A array [2].
- specific tests of Front End Electronics (FEE) circuit prototypes developed to equip the detector (Section 3). In this case, the flux of particles is expected to spoil the good working of FPGA circuits used to control several functions of the system.

2 The radiation effects in V0 scintillating materials

2.1 Expected doses and radiation effects

The choice of the elements listed above (scintillating plastic and WLS fibres) was mainly dictated by the time resolution performance of the counter for the detection of one MIP

(Minimum Ionizing Particle). Their hardness to radiations was not a decisive criterion. The radiation doses estimated during 10 years of operation through the V0 arrays are of the order of 200-300, 50, 20, and 10 krad for the most irradiated elements of rings 1 to 4 respectively [3, 4]. Several tests of light production degradation under radiations can be found in the literature for several scintillating plastics, WLS and optical fibres. Starting from these data or their extrapolation, we can estimate the signal reduction of the V0 counters in the particular ALICE environment.

The BC404 scintillator (decay time, 2 ns; peak emission, 408 nm; attenuation length, 1.7 m) was tested in radiation conditions up to 3 Mrad. A light reduction of about 5% was measured for a dose of 200-300 krad from a Cs^{137} radioactive source [5]. As a consequence, the degradation of the BC404 signal (factor of reduction **a**) does not seem to be a major problem for the ALICE experiment, even for the most exposed elements of the V0C array.

More drastic is the effect of radiation on the light emitted by the WLS fibres. Two effects must be considered here. The first one (factor of reduction **b**) is the brightness/transparency deterioration localized in the part of the fibres where the wavelength shift takes place. The absorbed doses are similar to the ones experienced by the scintillating plastic, namely the ones given above for each ring of the V0A and V0C arrays. BCF91/Y11 fibres show less than 10%/5% of light attenuation under 200-300 krad doses [6]. Although tested, the Y11 fibre was not selected because, due to its large decay times (8 ns), it provides a poor time resolution for the MIP detection (see [1] for a comparison of the Y11 and BCF9929A responses). For the same reason, the BCF91 was not tested and the BCF9929A was chosen. Unfortunately, its radiation hardness is worse as compared to the one of the BCF91 [7]. A relative light yield reduction (BCF9929A/BCF91) of 20% at 200 krad can be foreseen [8], leading to an absolute loss of about 30% for BCF9929A. Therefore, the WLS fibre seems to show a much larger radiation ageing than the scintillator. The second effect is the reduction of the mean path of the photons (factor of reduction **c**) in the part of the fibres exposed to radiations between the scintillating plastic and the connector. We evaluate these radiation doses to be 50, 20, 10, and 6 krad at the external radius of each ring, then decreasing very rapidly [3]. For the fibres of ring 1 counters, the dose is only 30 krad at 10 cm. Measurements of transparency were carried out with Y11 and BCF92 [9]. For a 30 cm long fibre, the length of the fibres guiding the light from ring 1 elements to connectors, and a 500 krad dose, the light yield attenuation by the BCF92 fibres is approximately 40%. The BCF9929A fibre, which is chosen for the V0 detector, has characteristics similar to the BCF92 one. With the radiation doses received in ALICE, we could expect a light attenuation not larger than 5%. The resulting radiation effect on the WLS fibres will be the loss of brightness added to the loss of transparency.

The optical fibres are exposed to radiations too (factor of reduction **d**). The dose can be very approximately evaluated starting from the results shown in [3]. At 44 and 32 cm in the V0A and V0C location respectively, the dose is about 3 krad for 10 years of data taking. A measurement with a 5 meter long Kuraray multi-clad fibre [10] shows that the absorption of a 500 nm wavelength light is about 15% for the dose above. This should indicate that, in our setup, the optical fibres are not degraded as compared to the WLS fibres.

To summarize, we can expect a loss of light yield not larger than 40% during the 10 years of ALICE operation even without taking into account the partial recovering of the scintillation during the yearly shut down of the experiments. In other words, this 40% reduction, sum of the several contributions listed above, must be considered as an extreme upper limit. The numbers given above are very rough estimations. Specific measurements presented below give a more precise knowledge of radiation effects on the actual V0 detector elements. The management of the detector along the time (10 years of LHC beam is the basic period to be considered) can thus be refined.

2.2 Setup of the irradiated scintillating device

We measured the evolution of the signal given by a counter of the ring 1 (the most affected by radiations) as a function of the radiation dose received by the scintillator alone (**a**), the WLS fibre coupled to the scintillator with optical cement (**b**), the WLS (**c**) and optical (**d**) fibres in their part used for the transport of the light. **a**, **b**, **c** and **d** are the fraction of initial light surviving after an irradiation of the counter. A sketch of the device is shown in Fig. 2. It was made of the ring 1 element coupled with four layers of nine WLS fibres (50 cm long) glued along its two radial edges. An aluminium plate of 2 cm in thickness set in front of the counter was used to define an area of radiation exposure (2 x 3 cm^2). One photo-multiplier was connected to each WLS fibre bundle directly or through 50 cm long clear fibre bundle. PMT1, PMT2, PMT3 and PMT4 were used to measure the output signal affected by radiations. They measured respectively the light yield distributions **a**, **ab**, **ac** and **abd** after each stage of irradiation (Fig. 2).

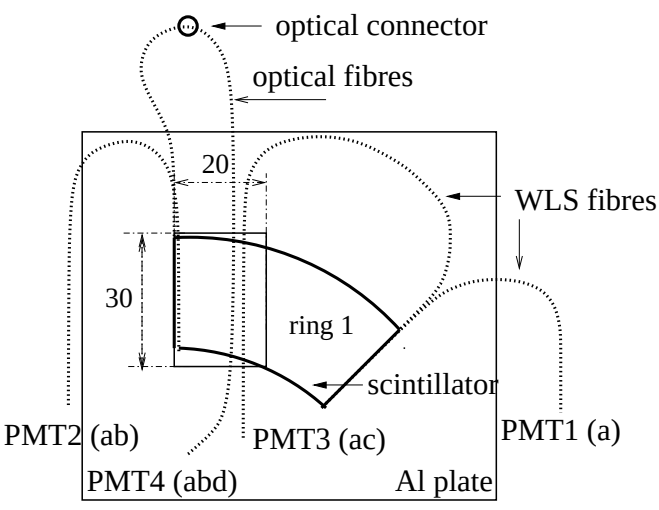

Figure 2: Front sketch (left) and picture (right) of the irradiated counter.

2.3 Light measurements

We used a 60 MeV proton beam uniformly distributed within the window mentioned above. The beam had a cylindrical envelope, meaning that each proton trajectory was perpendicular to the counter entrance face. For a current of 1 nA in the accelerator ($6.25\ 10^9$ p.sec^{-1}), the percentage of protons per cm^2 within the collimator was evaluated to about 1.3%. It corresponded to $81.25\ 10^6$ p.sec^{-1}.cm^{-2}. The initial signal, before any radiation effect, simulated about 7 MIPs as expected in ALICE.

After each exposure corresponding to a certain time of irradiation not longer than 45 minutes (time needed for a 100 krad dose), we measured, during about 15 minutes, change of the setup included, the PMT signals provided by protons crossing the counter. Therefore, one measurement consisted of one irradiation followed by one signal measurement. This procedure lead to have two setups (Fig. 3), the first one for the irradiation of the counter installed directly in the beam at the end of the beam pipe, the second one for the signal measurements themselves. For this step, the beam intensity was decreased to a few 10^5 p.sec^{-1} so that T1 and T2 PMTs used to provide the trigger could count the number of impacts. Several secondary signals were detected to control the radiation dose injected in the counter, and the beam intensity during the signal measurements: X-ray counting rate from an Ag foil by a NaI detector, scattered protons by the same Ag target, direct protons by the trigger detectors and Faraday cups inside the vacuum chamber of the beam and at the end of the test bench. The complete measurement took about 14 hours.

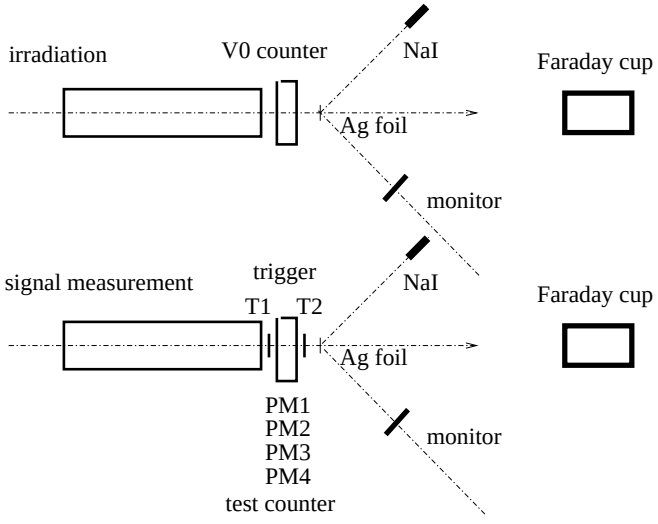

Figure 3: Setups for irradiation (top) and light measurements (bottom).

2.4 Results

The dose injected in a scintillator by one proton per cm^2 can be written as follows:

$$\Delta E \text{ x } 100 \text{ / } (1.02\ 10^{-3} \text{ x T x } 6.24\ 10^{12}) = 1.57\ 10^{-8}\ (\Delta E \text{ / T}) \text{ rad}$$

where ΔE is the energy loss in MeV, T the thickness in cm and $1.02\ 10^{-3}$ the mass in kg per cm^3 of the scintillating element.

The value of the ratio ($\Delta E/T$) depends on the irradiated zone of the counter. The figure 4 shows a cut view of the counter giving the size of the several components along the beam direction.

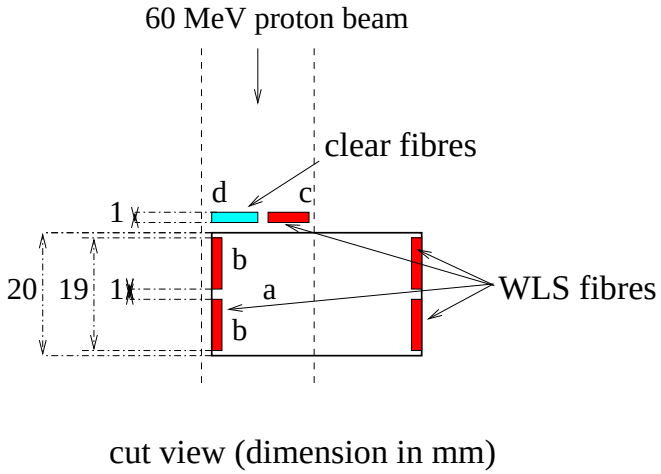

Figure 4: Cut view of the counter under test.

The $\Delta E/T$ ratio is constant for LHC energies (2 $MeV.cm^{-1}$), while it depends on the part of the counter for 60 MeV protons. The value of $\Delta E/T$ is given in Table 1 for each zone (Fig. 4) for which the residual light percentages after irradiation are called **a**, **b**, **c** and **d**. It means that in the present tests, for a 13.5 krad dose injected in the scintillator, 14.5, 11.7, 10 and 10 krad are respectively injected in the WLS fibres/cement volumes in the back and front parts of the scintillator, in WLS and optical fibres passing in the beam envelope inside the collimator.

	$\Delta E/T$ ($MeV.cm^{-1}$)	
Irradiated zone (**residual light percentage**)	LHC energies	60 MeV protons
scintillator (**a**)	2	13.5
WLS/cement (**b**), back part of the counter	2	14.5
WLS/cement (**b**), front part of the counter	2	11.7
WLS fibres in transmission (**c**)	2	10.0
optical fibres in transmission (**d**)	2	10.0

Table 1: Values of the $\Delta E/T$ factor.

The results of the light measurements are given in Fig. 5. The light yield distributions are normalized on the initial measurements (before irradiation). The relative uncertainties are evaluated to about 3%.

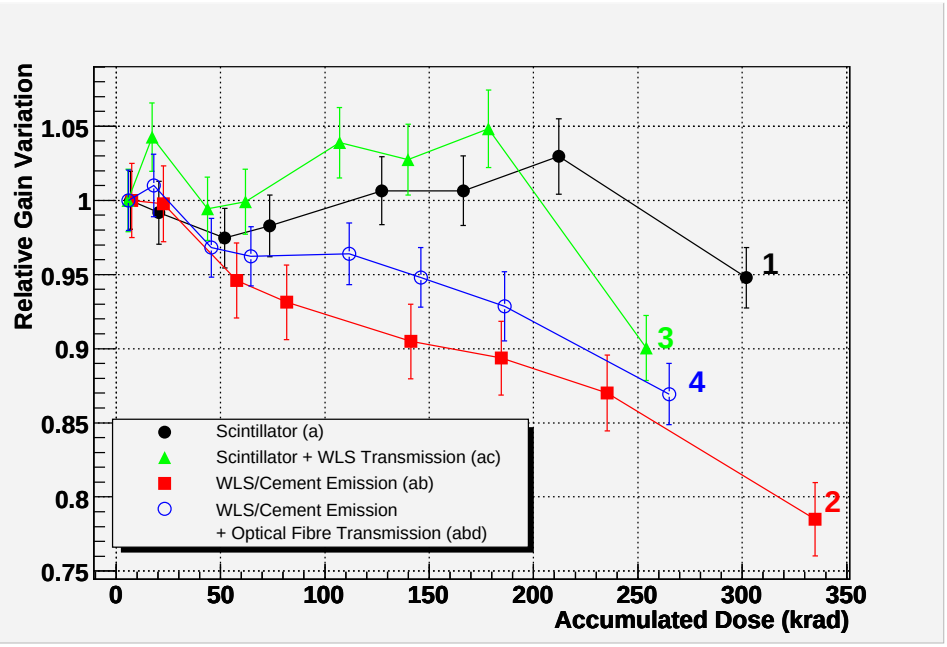

Figure 5: Relative light distributions as a function of the radiation dose injected inside several zone/elements constituting a V0 counter.

The distribution (1) is the light given by the scintillator as a function of the injected dose. The distribution is confined within the range 0.95-1.05, showing no perceptible effect up to 300 krad, except a possible beginning of degradation starting at this dose. This observation leads to conclude that the scintillator used for the V0 detector is not intrinsically subject to significant degradation for the expected dose of 200-300 krad. We thus can give the value 1 to **a**. This factor thus disappears from the other measured light yield distributions below.

The distribution (3) is the light from (1) going through the irradiated 3 cm long segment of the WLS fibres. This distribution gives the function of transmission **c** due to the irradiated WLS fibres. We measured no effect for a dose up to 150 krad and a clear attenuation from a dose of 200-250 krad. In the ALICE running conditions, the maximum dose expected during 10 years of exposure is not more than 30 krad close to the scintillating block and 3 krad at the level of the connector, with a mean value of 15 krad along the fibre of 30 cm in length. That corresponds to about 150 krad injected in 3 cm of fibre. That means the 250 krad dose of the test is larger than the expected dose in ALICE. We can thus deduce no significant loss of light coming from irradiation of WLS fibres alone is expected.

The distribution of light (2), namely the light from the WLS/cement volume close to the back face of the counter (**b**) as a function of the dose, is decreasing continuously from the initial value 1 to less than 0.8 at 350 krad. The production of light from WLS fibres embedded in optical cement is the most affected element of the V0 counter. 20%

of light attenuation has to be anticipated during the life time of ALICE for which a dose of 200-300 krad is foreseen. Nevertheless, this attenuation factor is smaller than the one extrapolated from the several measurements found in the literature (Section 2.1).

Finally, the distribution (4), plotted as a function of the dose injected in the WLS/cement volume close to the front face of the counter, shows the light emitted from the volume above (**b**) passing through an irradiated 3 cm long segment of the optical fibres. This distribution is given by the product **bd**. Any effect of radiation on optical fibre transmission should be reflected by a distribution (4) with a slope different from the one of the distribution (2). No such an observation is shown by the results. The optical fibre will thus be not greatly degraded during the ALICE experiment. Moreover, the radiation dose anticipated in the optical fibres (a few krad) is extremely low as compared to the dose injected in this test.

As a conclusion, and taking into account the incertainties of the measurements, we can expect a light attenuation due to radiation effects of about 25-30%. The major part of this degradation originates from the loss of brightness/transparency by the WLS fibre/cement assembly (**b** = 20%). The residual contribution (**a** + **c** + **d** = 5-10%) comes from secondary effects on the scintillator, and on the light transmission by the WLS/optical fibres used as light guides to the photo-multipliers. Moreover, a recovering of the scintillation cannot be significant during the total time of the measurements (14 hours). That means that the 25-30% effect should be considered as a maximum.

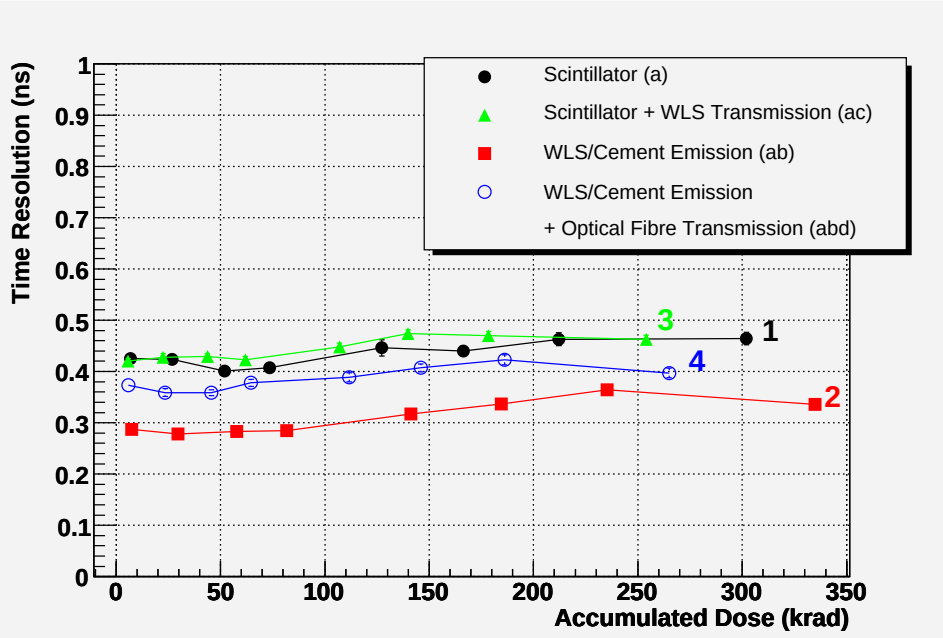

Figure 6: Time resolution distributions as a function of the radiation dose injected inside several zone/elements constituting a V0 counter.

The results of the time resolution measurements (σ_{time}) are given in Fig. 6. The vertical bars represent the r.m.s. of the time distributions. The values depend mainly on the photo-multiplier used on each channel. They are all confined in the range 300-500 ps. No significant dependence of this parameter with the radiation dose is measured. It has to

be recalled that the detected charges are large in the present test. A weak attenuation of the signal does not influence the timing performance of the counters. The situation should be much less favourable for the detection of the MIP in the ALICE conditions where we should observe a degradation of the resolution when the radiation dose increases.

3 The particle flux effects on V0 electronics circuits

3.1 The particle flux on the V0 electronics device

Radiation levels at the electronics rack location (B18) are very low [4]. As a consequence, the relevant quantity to be considered for the electronics devices is the flux of particles. About 1.93 10^6 charged hadrons and 9.82 10^5 neutrons of energy above 20 MeV are expected per cm^2 during 10 years in this area of the experiment. The test with 60 MeV protons was dedicated to evaluate the number of errors induced in the FPGA circuits used in the boards of the V0 Front End Electronics.

3.2 Setup and irradiated electronics devices

The setup of the irradiation test is shown in Fig. 7. A collimator of 1.5 x 1.5 cm^2 limited the beam to the circuit to be tested. T1 (T2) counted the protons (the scattered protons by the Ag foil) when the flux was low, whereas T2 alone allowed to measure the proton flux when it was high. Four independent measurements were carried out at different proton flux, namely 4.3 10^5, 10.0 10^5, 47.5 10^5 and 187.6 10^5 protons per cm^2.

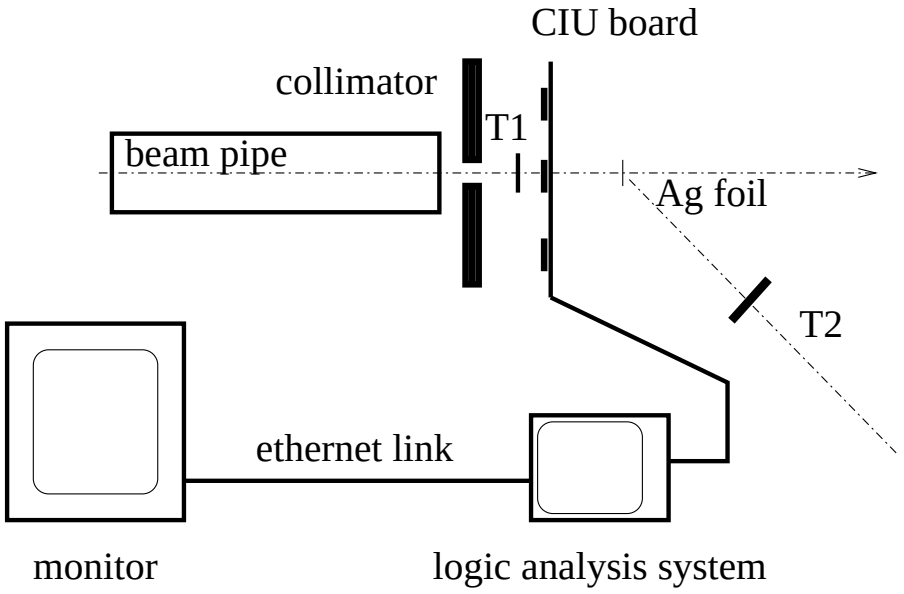

Figure 7: Setup of the electronics radiation test.

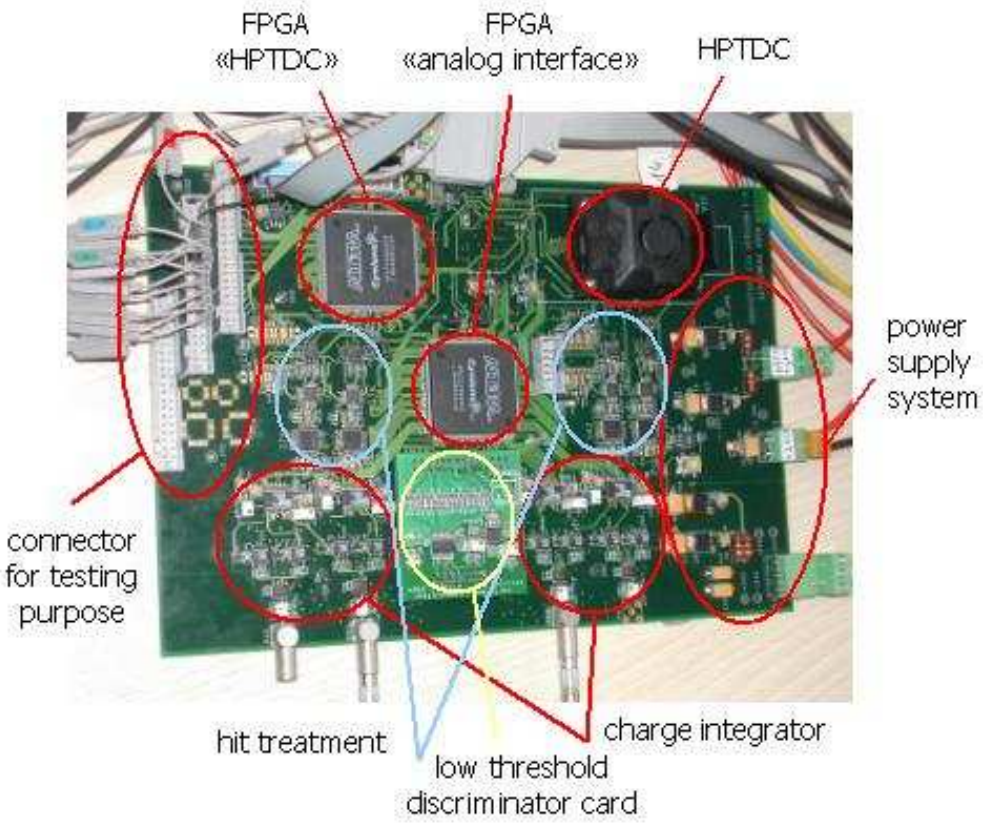

Figure 8: CIU board overview.

The CYCLONE EP1C12 FPGA radiation test was performed with a CIU prototype board (Fig. 8). The irradiated FPGA was the one named "analog interface" used for the charge integration management. The FPGA named "HPTDC", normally used to control the HPTDC circuit, was used here to supervise the radiation test. The programs of both FPGAs were thus completely modified in order to fulfil the following functions:

1. For the "analog interface" FPGA:

   - RAM implementation: one RAM of 26000 words of 8 bits was implemented, namely 86% of the memory bits of the EP1C12 (the normal application uses about 10% of the total memory bits).
   - Shift register implementation: two shift registers (6000 bits each) were implemented, namely 99% of the logic elements of the EP1C12 (the normal appli-

cation uses about 10% of the total logic elements).

- Activation of the error detection Cyclic Redundancy Check (CRC) feature of the EP1C12. The CRC was computed by the Quartus II software (used for the configuration of the FPGA), and downloaded into the FPGA as a part of the configuration bit stream. The FPGA stored the CRC in the 32-bit storage register at the end of the configuration mode. The FPGA re-calculated the CRC based on the contents of the device and compared it to the 32-bit storage register. The CRC ERROR pin was driven low until an error occured (the CRC calculation time was about 3.5 ms).

2. For the "HPTDC" FPGA:

- A scanning function for the memory of the "analog interface" FPGA. This function fulfilled the memory of the "analog interface" FPGA with logical "0" data at initialisation, and controlled the memory content during the radiation test by a cyclic reading. A memory error was considered when at least 10 bits of the complete memory were swapped from "0" to "1". When a memory error occured, a complete rewriting was performed and the cyclic reading restarted, and so on until the end of the test.
- A scanning function for the shift registers of the "analog interface" FPGA. This function fulfilled one of the shift register with logical "0" and the other ones with logical "1". This function also controlled that the data at the outputs of the shift registers corresponded to the sent ones. A register error was considered in case of one mismatch between input and output data.
- A scanning function for the CRC of the "analog interface" FPGA. A CRC error was considered when the CRC output of the "analog interface" became active. In such a case an automatic reconfiguration of the "analog interface" FPGA was performed and the scan function restarted and so on until the end of the test.

The radiation test consisted in counting each type of errors.

3.3 Results

The results are shown in Table 2.

Run number	Proton flux ($p.sec^{-1}.cm^{-2}$)	Time (sec)	Number of protons	Config. error	Register error	Memory error	CS cm^2
1	$4.3\ 10^5$	3300	$1419\ 10^6$	7	1	0	$5.63\ 10^{-9}$
2	$10.0\ 10^5$	1419	$1424\ 10^6$	26	0	0	$1.83\ 10^{-8}$
3	$47.5\ 10^5$	264	$1254\ 10^6$	25	0	0	$1.99\ 10^{-8}$
4	$187.6\ 10^5$	64	$1200\ 10^6$	19	0	0	$1.58\ 10^{-8}$

Table 2: Errors recorded as a function of the particle flux on the FPGA chip EP1C12.

The cross-section (CS) given in the last column is calculated with the relation:

$$\text{CS} = \text{Nb SEU} / (\text{flux x time}) = \text{Nb SEU} / \text{fluence}$$

where SEU is the Single Event Upset provided by the flux of particles through the FPGA electronics component.

A first remark is that we have for the EP1C12 FPGA a cross-section ($2\ 10^{-8}$ cm^2) close to the one of the EP1C20 FPGA ($3.3\ 10^{-8}$ [11]) which is built in the same technology but with larger number of logical elements (a factor 1.66 above) and RAM bits (a factor 1.23 above). The results are very similar if we compare the cross-sections of one logical element for each FPGA: about $1.658\ 10^{-12}$ cm^2 for the EP1C12 FPGA (12060 logical elements) and $1.645\ 10^{-12}$ cm^2 for the EP1C20 FPGA (20060 logical elements).

Assuming a hadron (>20 MeV) fluence of $1.93\ 10^6$ cm^{-2} during 10 years in the electronics rack location [4], a SEU cross section for the EP1C12 FPGA of $2\ 10^{-8}$ cm^2 (present measurement), a SEU cross section for the EP1C20 FPGA of $3.3\ 10^{-8}$ cm^2 [11], we calculate for the 24 EP1C12 and the 2 EP1C20 FPGAs used in the V0 complete electronics system a number of SEU as follows:

$$\text{Nb SEU} = (\textstyle\sum_{FPGA}\text{CS}) \text{ x fluence} = (24 \text{ x } 2\ 10^{-8} + 2 \text{ x } 3.3\ 10^{-8}) \text{ x } 1.93\ 10^6 = 1.05$$

In conclusion, all the FPGAs of the V0 Front End Electronics will experience no more than 1 SEU every 10 years of ALICE running, and even much less since their actual use will concern only 10% of their capacity.

4 Conclusion

A control of radiation effects on several elements of the ALICE V0 detector was carried out with a proton beam of 60 MeV delivered by the Jyväskylä RADEF facility.

It was observed that a moderate light attenuation can be expected during the 10 years of the ALICE experiment. A reduction of the order of 25-30% was measured for a dose of 350 krad. This light degradation is mainly due to radiation effects on the WLS fibres embedded in optical cement. A possible compensation of this loss of signal can be envisaged through a gain adjustment of the photo-multipliers. Moreover, the construction of spare rings 1 and 2, the rings the most exposed to radiations, will allow to secure the permanent utilization of the V0 detector.

Concerning the effect of the flux of particles expected in the electronics system location, it was observed that the adopted FPGA chip could experience only one Single Event Upset during the 10 years of the ALICE experiment. Although negligible, the chips will be periodically monitored (CRC) and, in case of error, automatically reloaded from flash.

Acknowledgments

The authors are very grateful to W. Trzaska, V. Lyapin, T. Malkievicz for their invaluable help before, during and after the test period, A. Virtanen, H. Kettunen, A. Pirojenko for their warmly welcome and efficient contributions for the control of the accelerator, F. Formenti, L. Musa for their precious advices on the electronics irradiation method and analysis, D Essertaize, G. Gelin, S. Vanzetto and the workshop team for their efficient participation to the V0 counter construction. Finally, BC, JYG, RT, WT and YZ had the possibility of doing the tests thanks to W. Trzaska, R. Julin, the support of the Jyväskylä laboratory and the EURONS contract 506065 (experiment I73).

References

[1] ALICE Collaboration, CERN-LHCC-2004-025, "Technical Design Report on Forward detectors: FMD, T0 and V0", ALICE TDR 011, 10 September 2004.

[2] A. Sandoval *et al.*, V0 Production Readiness Review Report, July 11, 2005.

[3] F. Carminati *et al.*, PPR Vol 1, Phys. G: Nucl. Part. Phys. 30 (2004) 1517.

[4] http://alicedcs.web.cern.ch/AliceDCS/ElectrCoord/Documents/

[5] V. Bezzubov *et al.*, "Fast Scintillation Counters with WLS Bars", FERMILAB-Conf-98/020.

[6] E. Tarkovsky, NIM A379 (1996)515.

[7] BICRON, private communication.

[8] S. Barsuk *et al.*, "Radiation damage of LHCb electromagnetic calorimeter", LHCb 2000-033.

[9] G. Britvich *et al.*, "The HCAL Optics Radiation Damage Study", LHCb 2000-037 HCAL.

[10] K. Hara *et al.*, NIM A411(1998)31.

[11] "Radiation Results of the SER test of Actel, Xilinx and Altera FPGA instances", IROC TECHNOLOGIES, Ref: GRE_2_Actel_SERTEST_DEC_03_ENG_TR_008